Dewetting near the Glass Transition: Transition from a Capillary Force Dominated to a Dissipation Dominated Regime

Pascal Damman,[1,*] Nancy Baudelet,[1] and Günter Reiter[2,†]

[1]*Laboratoire de Physicochimie des Polymeres, Université de Mons Hainaut, 20, Place du Parc, B-7000 Mons, Belgium*
[2]*Institut de Chimie des Surfaces et Interfaces, CNRS-UHA, 15 rue Jean Starcky, BP 2488, 68057 Mulhouse CEDEX, France*

(Received 18 July 2003; published 19 November 2003)

Dynamics and corresponding morphology of dewetting of thin polystyrene films at temperatures close to the glass transition were investigated by measuring simultaneously dewetted distance and width of the rim. Comparing the opening of cylindrical holes with the retraction of a straight contact line revealed (i) a drastic influence of the geometry (planar or radial symmetry) on the dynamics at early stages, (ii) a new logarithmic dewetting regime, and (iii) transitions between four dewetting regimes clearly indicated by changes in the shape of the rim. The complete dewetting scenario can be understood as an initial dominance of capillary driving forces, which is progressively overtaken by dissipation related to the increasing size of the rim.

DOI: 10.1103/PhysRevLett.91.216101 PACS numbers: 68.60.–p, 61.41.+e, 68.15.+e, 83.50.–v

A liquid film which is forced to cover a nonwettable substrate is not stable and will dewet this substrate. Dewetting starts by forming a three-phase contact line where substrate, film, and environment (e.g., air) meet. The dynamics of this contact line is determined by the counteraction of capillary driving forces (action) and dissipation (reaction of the moving part). One or more dissipation mechanisms may be at work which depend on substrate-fluid interaction and the nature of the fluid (via parameters such as the viscosity, relaxation rates, elasticity, ...). For cases dominated by dissipation, e.g., polydimethylsiloxane (PDMS) on solid substrates, the dewetting velocity is controlled by consumption of capillary energy either at the three-phase contact line (no-slip boundary condition) [1] or at the solid/fluid interface (slip boundary condition) [2–4]. If dissipation is weak, capillary forces may dominate and lead to exponential growth of dewetting holes [5]. Combining these opposing cases, Brochard-Wyart *et al.* [5] predicted a sequence of three different characteristic regimes.

The dewetting of freestanding polystyrene (PS) films was reported by Dalnoki-Veress *et al.* [6]. Although the dynamics of the hole opening followed the *viscous bursting* dynamics previously proposed by Debregeas *et al.* for suspended PDMS films [7,8], an additional nonlinear viscoelastic effect was observed. More recently, one of us showed that dewetting of thin polymer films, which were supported by a silicon (Si) wafer coated with a PDMS layer, could be achieved at temperatures very close to the glass transition [9]. Contrary to previous observations, the dewetted "glassy" polymer was collected in a highly asymmetric rim, differing strongly from the more symmetric shape which minimizes the Laplace pressure in the rim. Different theoretical works, based on opposing assumptions for the dissipation mechanism (shear thinning [10], strain hardening [11], and viscoelastic behavior [12]), succeeded all in reproducing the formation of these asymmetric rims.

In this Letter, we present new experimental findings about the dynamics of the dewetting process for the same system as in Ref. [9] which resolve the "mystery" of why a large variety of different behaviors are observed. The detailed knowledge of dynamics and morphology of the rim, together with other relevant parameters such as temperature or molecular weight, is a basic requirement to solve the controversy about which mechanisms are controlling dewetting near the glass transition.

For the experiments presented here, we used thin polystyrene films (PS, molecular weight $M_W = 110$ and 950 kg/mol, and index of polydispersity $I_p = 1.05$) of different thicknesses (h_0) between 20 and 100 nm (as measured by ellipsometry) on top of silicon substrates. To obtain large capillary forces, the substrates were coated with a layer of adsorbed PDMS ($M_W =$ 90 kg/mol, $I_p = 1.96$, layer thickness about 4 nm). The irreversibly adsorbed PDMS layers resulted from annealing spin-coated films on hydroxylated (plasma cleaned) silicon wafers at 150 °C for 5 h under vacuum [3,4]. PS films were prepared from toluene solution spin coated directly onto the PDMS-coated Si wafers.

Isothermal dewetting of thin PS films was followed in real time, t, by optical microscopy. In addition to the dewetted distance, the width of the rim also was measured accurately during the fluid retraction for various experimental conditions, i.e., temperature, molecular weight, and dewetting geometry. As shown previously, the opening of holes and the dewetting of edges, corresponding to radial and planar symmetries, respectively, can be easily resolved by optical microscopy [3,4]. The displacement of a straight three-phase contact line was made possible by breaking the sample in two parts, a process used previously [3,4]. We followed the hole opening and edge dewetting versus time with a CCD camera, the image being analyzed with the ImageJ software [13].

As reported previously for freestanding [6–8] and supported films [9,14], the first stages of hole opening in

polymer dewetting are characterized by an exponential growth of the hole radius, R (Fig. 1): $R(t) = R_0 e^{t/\tau}$, where τ is a characteristic time varying with film thickness and molecular weight [6–8].

This mode of hole growth corresponds to the regime dominated by capillary forces for which all the liquid removed from the growing hole is homogeneously spread throughout the remaining film, i.e., no rim is observed in this regime. The exponential growth arises from the increase of the capillary energy with the hole radius [7].

For dewetting from the edge, such an exponential growth is not expected [15] since the length of the three-phase contact line is constant and maximum (for planar symmetry: $R = \infty$). The edge dewetting velocity therefore attains almost instantaneously a high value.

As shown in Fig. 1, a transition from exponential growth to another regime was observed during hole opening. This transition can be characterized by a change of the dynamics and by the formation of a rim as confirmed by optical microscopy. Such a transition is expected at a critical radius, R_C, which, for the case of *viscous* dissipation at the substrate film interface (i.e., slippage), is determined by the hydrodynamic extrapolation length and the film thickness [5]. Although a different dissipation mechanism is at work, our experiments suggest that R_C is also affected by the properties of the PDMS-coated substrate.

In the following, we focus on the regimes governed by the buildup of a rim and examine the influence of dewetting geometry on the dynamics. Figure 2 shows a selection of micrographs recorded during isothermal dewetting of a hole and an edge, observing both simultaneously. The dewetted distance, D, the radius of a hole, R, and the rim width, W, were easily measured utilizing interference contrast (a height resolution of a few nm can be achieved by reflection optical microscopy). The detailed evolutions of R, D, and W are shown in Fig. 3 together with the dewetting velocity V computed as dR/dt (or dD/dt) from the experimental data.

Clearly, the retraction dynamics of the edge and the hole are significantly different. For the edge, V decreased right from the start as $V \propto t^{-1}$, while two distinct regimes ($V = \text{const}$, followed by $V \propto t^{-1}$) were found for the opening of a hole. Both dynamics converge for long times. The constant velocity regime found for the opening of a hole reminds us of viscous dissipation in the no-slip situation observed by Redon *et al.* [1], where V is constant because both the driving capillary forces and the viscous force are constant in time. V is given by $V = \frac{1}{6}\frac{\gamma}{\eta}\frac{1}{L}\theta^3$, where γ, η, L, and θ are the polymer/air free surface energy, the film viscosity, a logarithmic factor due to the dissipation in the wedge, and the equilibrium contact angle, respectively.

With this equation and appropriate parameters ($\gamma = 30\ \text{mN/m}$, $\eta_0 = 2 \times 10^6\ \text{Pa s}$, $L \sim 10$, and $\theta \sim 45°$), we calculated a velocity of $10^{-4}\ \mu\text{m s}^{-1}$, which is about 2 orders of magnitude smaller than the observed value of $V \sim 10^{-2}\ \mu\text{m s}^{-1}$ (see Fig. 3). The discrepancy indicates that a different dissipation mechanism is at work, e.g., related to a shear thinning behavior. For high molecular weight polymers, a severe decrease of the viscosity could be achieved during shear [16], which, in turn, would induce an increase of the dewetting velocity.

In order to shed more light on the origin of the different dewetting behaviors found for the two geometries, we examined the shape of the rim more closely. The evolution of W versus time [Fig. 3(a)] strongly supports the existence of two distinct regimes during the process of rim buildup. This holds for both geometries. First, up to a maximum value $W_{\max}$, a rapid growth of the rim width was observed. Surprisingly, this "formation" regime was followed by a second regime characterized by an almost constant (or slightly decreasing) rim width. The transition point between these two growth regimes coincided with the intercept of the velocity of edge and hole [t^* in Fig. 3(c)]. From additional experiments (not shown here), time and dewetted distance characteristic of this transition were found to be highly

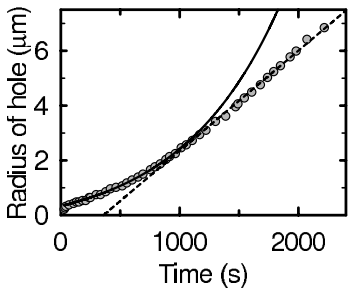

FIG. 1. Time dependence of the hole radius during the first stages of dewetting for a PS thin film supported by a PDMS brush ($M_W = 110\ \text{kg/mol}$, $h_0 = 69\ \text{nm}$, $T = 125\ °\text{C}$).

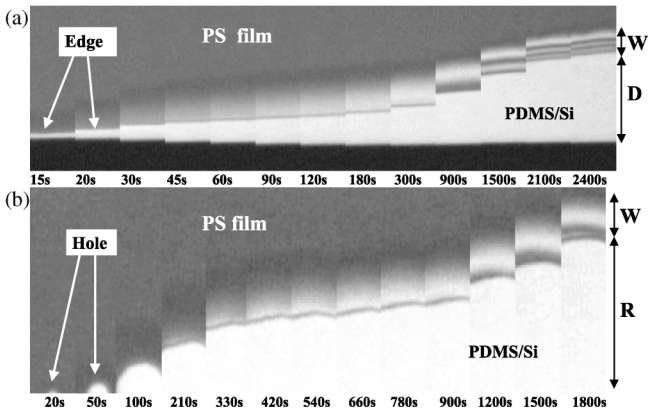

FIG. 2. Optical micrographs of a section recorded during the dewetting of a PS thin film deposited on a PDMS (thickness 4 nm) coated Si wafer (PS $M_W = 110\ \text{kg/mol}$, $h_0 = 69\ \text{nm}$, $T = 125\ °\text{C}$): (a) edge-planar symmetry; (b) hole-radial symmetry.

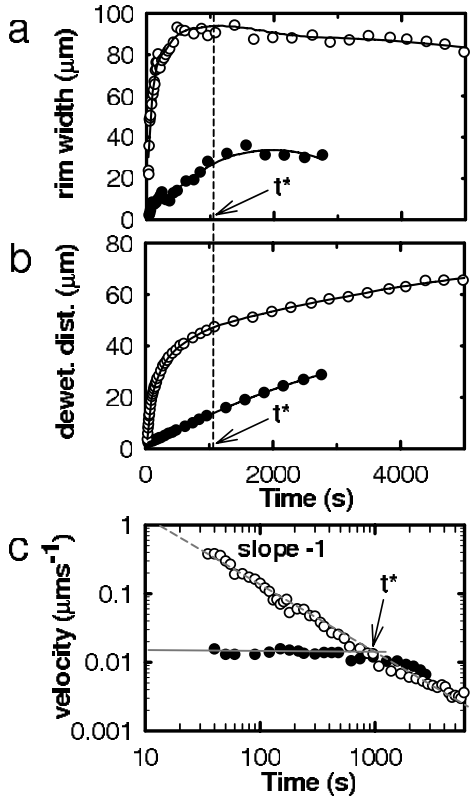

FIG. 3. Evolution of (a) the width of the rim, W, (b) the dewetted distance, R or D, and (c) the dewetting velocity, V, versus time, simultaneously measured for a supported thin PS film ($M_W = 110$ kg/mol, $h_0 = 69$ nm, $T = 115\,^{\circ}$C). Hollow and filled symbols refer to planar (edge) and radial (hole) symmetry. The dashed line in the logarithmic plot of V versus t corresponds to a slope of -1.

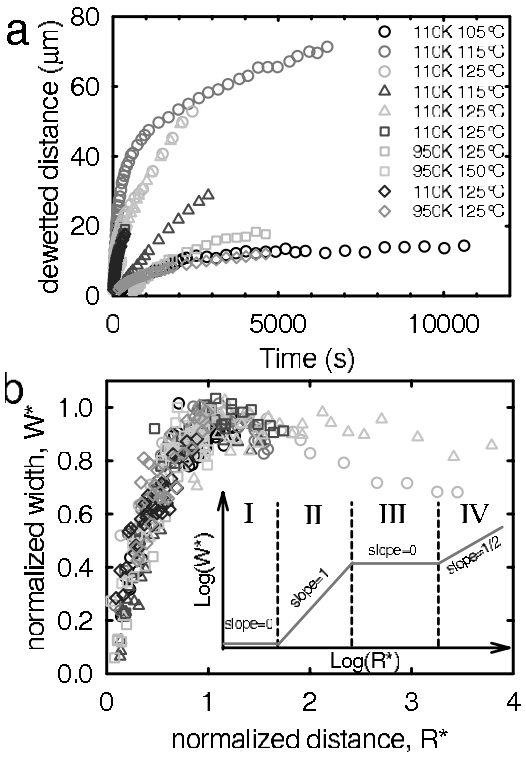

FIG. 4. (a) Time dependence of the dewetted distance or hole radius measured for various thin PS films supported by a PDMS-coated Si wafer. (b) Normalized plot of the rim width, W^*, versus the dewetted distance, R^*, for the different dewetting experiments. A scheme of the normalized plot, $\log(W^*)$ versus $\log(R^*)$, for the four dewetting regimes is given as an inset. M_W and T are as indicated in the figure. Film thicknesses: edge geometry, circles (69 nm) and squares (39 nm); hole geometry, triangles (69 nm) and diamonds (39 nm).

sensitive to temperature and molecular weight (i.e., viscosity) but rather insensitive to film thickness.

A selection of results obtained for experiments performed at different temperatures, for different molecular weights, thicknesses, and dewetting geometries, are compiled in Fig. 4(a). As can be seen, the dynamics strongly depended on the experimental conditions (i.e., the plot appears rather complex). However, when normalizing these data by $W_{\max}$ and the corresponding dewetted distance, $R(W_{\max})$, we obtained a $W^* = W/W_{\max}$ versus $R^* = R/R(W_{\max})$ master curve, indicating that all these experiments were controlled by the same dissipation mechanism(s) [Fig. 4(b)].

As volume is conserved, this W^* versus R^* plot is a clear indicator for changes of the shape of the rim. In the first regime, we observed that the rim width increased linearly with the dewetted distance. This linear relationship, also found in [9], indicates that the unique asymmetric rim shape holds for this first regime (i.e., growth is homothetic). At the transition, corresponding to $R^* = W^* = 1$, we observed a distinct change in behavior. While the dewetted distance still increased continuously, the rim width remained constant for the holes and even decreased slightly for edges. As the volume of the rim still increased (i.e., the material removed by dewetting increased), this could be achieved only by a change in the shape of the rim, from a highly asymmetric to a more symmetric rim. Such conclusion is supported by a direct microscopy observations (Fig. 2). Although at later times the rim width is constant, the increase in the number of interference fringes suggests that the rim became increasingly more symmetric (e.g., 1500–2400 s for the edge). Eventually, the known parabolic (no-slip) or self-affine (slip) shapes will be found, obeying $W \propto R^{1/2}$ [17]. The four dewetting regimes are illustrated in the $\log(W^*)$ versus $\log(R^*)$ plot given in Fig. 4(b). The master curve plotted from the normalized experimental data corresponds to regimes II and III of the scheme [Fig. 4(b)].

Finally, we can rationalize and summarize all our experimental observations in the generic scheme given in Fig. 5, which describes the four regimes of the overall dewetting behavior of nonlinear viscoelastic fluids such as PS melts close to the glass transition.

At the two extremes, we find a regime dictated by the capillary driving forces (exponential growth) and a

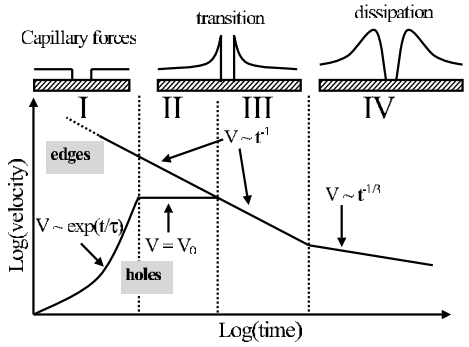

FIG. 5. Schematic view of the overall dewetting behavior of nonlinear viscoelastic fluids together with their associated rim shapes.

regime dominated by viscous dissipation in the rim ($R \propto t^{2/3}$ and $V \propto t^{-1/3}$), respectively. In between these boundary cases, we have observed two distinct regimes controlled by increasing dissipation, related to the buildup of a rim of characteristic shape. In the first of these regimes, geometry is essential. For the planar geometry, the driving force is constant right from the beginning. Thus, during the buildup of the rim and the continuous increase of dissipation, the velocity is decaying linearly in time. In the case of a growing hole, the increasing driving force proportional to the perimeter is balanced by increasing dissipation, resulting in a constant velocity. At later stages, dissipation is still increasing but is not compensated (fully) by an increase in the driving force. Consequently, the dewetting velocity is decreasing in time. Once the rim has reached its final shape [either parabolic (no-slip) or self-affine slightly asymmetric (slip)], the dewetting velocity is either constant [1] or decreasing as $V \propto t^{-1/3}$ [2–4].

In summary, the major features of dewetting characterizing the transition from an initial regime dominated by the capillary driving forces to dissipation dominated regimes are as follows: (i) Initially the dewetting geometry has a strong influence. (ii) As dissipation becomes important, a highly asymmetric rim is formed. Here, we note that the actual dissipation mechanism has no or little influence on the shape of the rim; see the opposing assumptions made in [10–12], all resulting in similar shapes of the rim. (iii) The transition from a highly asymmetric to a more symmetric shape of the rim characterizes the transition to dissipation dominated dewetting. (iv) Initially, the observed dewetting velocity is larger than what is expected according to the no-slip model. (v) At constant driving force, a logarithmic growth law reflects the continuous increase of dissipation proportional to the dewetted distance. We note that the complete set of these basic features such as logarithmic evolution laws or the existence of a shape transition in the course of dewetting are not yet described by the "state of the art" theories [10–12]. Thus, we hope that these new experimental results on the dewetting of viscoelastic fluids will initiate further theoretical work.

This work was supported by the Belgian National Fund for Scientific Research (FNRS). The authors thank Florent Saulnier, Elie Raphaël, Didier Villers, and Roberto Lazzaroni for stimulating discussions. P. Damman is a Research Associate of the FNRS.

*Electronic address: pascal.damman@umh.ac.be
†Electronic address: G.Reiter@uha.fr

[1] C. Redon, F. Brochard-Wyart, and F. Rondelez, Phys. Rev. Lett. **66**, 715 (1991).
[2] C. Redon, J. B. Brzoska, and F. Brochard-Wyart, Macromolecules **27**, 468 (1994).
[3] G. Reiter and R. Khanna, Phys. Rev. Lett. **85**, 2753 (2000).
[4] G. Reiter and R. Khanna, Langmuir **16**, 6351 (2000).
[5] F. Brochard-Wyart, G. Debregeas, R. Fondecave, and P. Martin, Macromolecules **30**, 1211 (1997).
[6] K. Dalnoki-Veress, B. Nickel, C. Roth, and J. Dutcher, Phys. Rev. E **59**, 2153 (1999).
[7] G. Debrégeas, P. Martin, and F. Brochard-Wyart, Phys. Rev. Lett. **75**, 3886 (1995).
[8] G. Debrégeas, P.-G. de Gennes, and F. Brochard-Wyart, Science **279**, 1704 (1998).
[9] G. Reiter, Phys. Rev. Lett. **87**, 186101 (2001).
[10] F. Saulnier, E. Raphaël, and P.-G. de Gennes, Phys. Rev. Lett. **88**, 196101 (2002).
[11] V. Shenoy and A. Sharma, Phys. Rev. Lett. **88**, 236101 (2002).
[12] S. Herminghaus, R. Seeman, and K. Jacobs, Phys. Rev. Lett. **88**, 056101 (2002).
[13] W. Rasband, http://rsb.info.nih.gov/ij.
[14] J. Masson and P. Green, Phys. Rev. Lett. **88**, 205504 (2002).
[15] M. Brenner and D. Gueyffier, Phys. Fluids **11**, 737 (1999).
[16] M. Doi, in *Materials Science and Technology*, edited by R. Cahn, P. Haasen, and E. Kramer (VCH Publishers, New York, 1993), Vol. 12, pp. 391–425.
[17] F. Brochard-Wyart, P. Martin, and C. Redon, Langmuir **9**, 3682 (1993).